Bioprocess Biosyst Eng (2011) 34:45–56
DOI 10.1007/s00449-010-0445-3

ORIGINAL PAPER

Modelling and simulation of steady-state phenol degradation in a pulsed plate bioreactor with immobilised cells of *Nocardia hydrocarbonoxydans*

K. Vidya Shetty · Dheeraj Kumar Verma · G. Srinikethan

Received: 21 November 2009 / Accepted: 30 May 2010 / Published online: 19 June 2010

Abstract A novel bioreactor called pulsed plate bioreactor (PPBR) with cell immobilised glass particles in the interplate spaces was used for continuous aerobic biodegradation of phenol present in wastewater. A mathematical model consisting of mass balance equations and accounting for simultaneous external film mass transfer, internal diffusion and reaction is presented to describe the steady-state degradation of phenol by *Nocardia hydrocarbonoxydans* (*Nch.*) in this bioreactor. The growth of *Nch.* on phenol was found to follow Haldane substrate inhibition model. The biokinetic parameters at a temperature of 30 ± 1 °C and pH at 7.0 ± 0.1 are $\mu_m = 0.5397\ h^{-1}$, $K_S = 6.445$ mg/L and $K_I = 855.7$ mg/L. The mathematical model was able to predict the reactor performance, with a maximum error of 2% between the predicted and experimental percentage degradations of phenol. The biofilm internal diffusion rate was found to be the slowest step in biodegradation of phenol in a PPBR.

Keywords Biodegradation · Immobilised cells · Pulsed plate bioreactor · Modelling · Biofilms

Symbols

a_{avg}	Average surface area of benzoic acid particle (m^2)
a_n	S^* at $x = 0$ for nth iteration
a_{n+1}	S^* at $x = 0$ for $(n + 1)$th iteration
A	Amplitude of pulsation (cm)
A_p	Total surface area of bioparticles in the reactor (m^2)
Bi	Biot number
C	Concentration of benzoic acid in the bulk liquid at the end of the run (kg m^{-3})
C^*	Solubility of benzoic acid in water (kg m^{-3})
d_p	Diameter of biomass free particle (m)
Da	Damkohler number
D_{eff}	Effective diffusivity of phenol in the biofilm ($m^2\ s^{-1}$)
D_w	Diffusivity of phenol in water ($m^2\ s^{-1}$)
f	Frequency of pulsation (s^{-1})
k_s	Liquid–solid mass transfer coefficient for phenol (m s^{-1})
K_I	Inhibition constant for phenol (kg m^{-3})
K_S	Monod constant for phenol (kg m^{-3})
K_I^*	Dimensionless inhibition constant for phenol
K_S^*	Dimensionless Monod constant for phenol
n	nth iteration
N_p	Number of bioparticles in the reactor
Q	Flow rate of synthetic waste water ($m^3\ s^{-1}$)
r	Radial coordinate in biofilm (m)
r_p	Radius of biomass free particle (m)
$R\ (S)$	Substrate consumption rate at any phenol concentration S (kg s^{-1})
$R\ (S_b)$	Substrate consumption rate at bulk phenol concentration (kg s^{-1})
$R\ (S_S)$	Substrate consumption rate at surface phenol concentration (kg s^{-1})
S	Phenol concentration in biofilm (kg m^{-3})
S_b	Phenol concentration in the bulk liquid (kg m^{-3})
S_I	Phenol concentration in influent synthetic wastewater (kg m^{-3})
S_{max}	Phenol concentration above which the growth is inhibited (kg m^{-3})
S_s	Phenol concentration at the surface of the biofilm (kg m^{-3})

K. V. Shetty (✉) · D. K. Verma · G. Srinikethan
Department of Chemical Engineering,
National Institute of Technology Karnataka Surathkal,
Srinivasnagar Post, Mangalore 575025, Karnataka, India
e-mail: vidyaks68@yahoo.com; vidyaks95@nitk.ac.in

S^* Dimensionless phenol concentration within the biofilm
$S^*_{x=1}$ Dimensionless phenol concentration at $x = 1$
W Total biomass in the reactor (kg)
x Dimensionless distance in the biofilm
$Y_{x/s}$ Observed yield coefficient (kg kg^{-1})
y^* Dimensionless concentration gradient in the biofilm
$y^*_{x=1}$ Dimensionless concentration gradient at $x = 1$

Greek letters

Δm Change in the mass of benzoic acid particle before and after the run (kg)
Δt Retention time of benzoic acid particle in the reactor (s)
δ Biofilm thickness (m)
$\eta_{external}$ External effectiveness factor
$\eta_{internal}$ Internal effectiveness factor
$\eta_{overall}$ Overall effectiveness factor
μ Specific growth rate of organism (s^{-1})
μ_m Maximum specific growth rate of organism (s^{-1})
ρ_b Biofilm density (kg m^{-3})
φ_s Thiele modulus for phenol

Introduction

Biological films formed by immobilised cells are commonly used in wastewater treatment (trickling filter, rotating disc contactor, fluidised bed bioreactor). Fixed film bioreactors exhibit properties that make them preferable to suspended cell systems for many bioprocess applications. These properties include extremely high cell concentration, enhanced cell retention due to cell immobilisation, increased resistance to toxic shock loading [1] and higher volumetric throughputs due to the independence of cell growth rate from reactor dilution rate. Many researchers have compared phenol removal using free cells and attached growth systems in laboratory experiments [2–6]. In all these cases, the efficiencies of immobilised cell systems were higher than those of the free or suspended cell systems. Superiority of immobilised cell systems was more pronounced at higher dilution rates. In addition, immobilised cell systems presented improved resistance to high phenol concentrations, whilst free cell systems presented strong toxicity and inhibitory effects for phenol concentrations less than 100 mg/L [7, 8]. Immobilisation eliminates the expensive processes of cell recovery and cell recycling. Besides these advantages, the use of immobilised microorganism has some disadvantages. One of the major problems of immobilisation is diffusion limitation. In such a case, the control of micro-environmental conditions is difficult because of the resulting heterogeneity in the system. With viable cells, growth and gas evolution can lead to significant mechanical disruption of the immobilising matrix [9]. A recent innovation in immobilised cell or fixed film bioreactors is the pulsed plate bioreactor (PPBR) with immobilised cells [10]. The advantages of this kind of bioreactor over other immobilised cell bioreactors are presented elsewhere[10]. Shetty et al. [10] have studied the performance of a pulsed plate bioreactor with immobilised cells for aerobic biodegradation of phenol and found its potentiality to be an efficient bioreactor for wastewater treatment.

In the present work, a steady-state model describing the biodegradation of phenol by immobilised *Nocardia hydrocarbonoxydans* (*NCh*) in a pulsed plate bioreactor was formulated on a similar basis as that employed for other types of immobilised cell reactors such as fluidised bed bioreactors [11–13]. No earlier reported work can be found in literature on the theoretical modelling of steady-state phenol biodegradation in a pulsed plate bioreactor with immobilised cells. The proposed steady-state model considered microbial growth described by Haldane substrate inhibitory kinetics, internal diffusion of substrate within the biofilm and external liquid–solid mass transfer resistance between the biofilm and completely mixed bulk liquid phase. The biokinetic parameters for the growth of *NCh*. on phenol as the sole carbon and energy source were determined. The novelty of the work lies in the use of a theoretical model to predict steady-state biodegradation in a pulsed plate bioreactor with immobilised cells of *NCh*. This microorganism is an actinomycete and was chosen for the degradation of phenol, as it was found to degrade phenol effectively and, being found in soil, it was more resistant to contamination [10, 14].

Development of a mathematical model

A steady-state model for the biodegradation of phenol by *Nocardia hydrocarbonoxydans*, immobilised on glass beads in a pulsed plate bioreactor, was developed.

Phenol conversion in a heterogeneous bioreactor such as PPBR with biofilms formed by the cells immobilised on glass beads can be described by three basic processes:

(1) Transport of oxygen from the gas phase into the bulk liquid;
(2) Transport of phenol, oxygen and other nutrients from the bulk liquid phase to the surface of the biofilm through a stagnant liquid film;
(3) Simultaneous diffusion and reaction of phenol, oxygen and other nutrients within the biofilm.

Process (1) was not considered in this work, as the concentration of dissolved oxygen in the reactor at steady

state was measured for all the experiments and was found to be constant at 5.6 ± 0.4 mg/L.

Figure 1 shows the hypothetical cross-sectional structure of the biofilm on a glass bead and the conceptual concentration profile at bioparticle interface and in the biofilm.

A pseudo steady state was assumed to exist in the PPBR when the concentration of phenol in the liquid phase remained constant for a period of 12 h.

The model was developed based on the following assumptions:

1. A pulsed plate bioreactor with packed bed of solids behaves like a CSTR with perfect mixing [10].
2. The pseudo steady state (steady state hereafter) implies that the rate of growth of biomass is equal to the rate of detachment by fluid shear, such that the biofilm thickness and overall biofilm density remain constant [11]. Hence, biomass loading is constant at steady state. The concentration profile of phenol across the liquid film and within the biofilm remains steady.
3. The "free" cells sloughed off the bioparticles (glass beads with biofilm) make only a negligible contribution to the overall degradation rate. This assumption was reasonable since the relative holdup of immobilised biomass in the reactor was very high, typically in the range of 1.822–6.776 kg m^{-3} compared to the negligible holdup of suspended biomass, which was in the range of 0.02–0.1 kg m^{-3}.
4. The biomass forms an even coating on the outside surface of the spherical glass particles and the biofilm is a homogeneous phase.

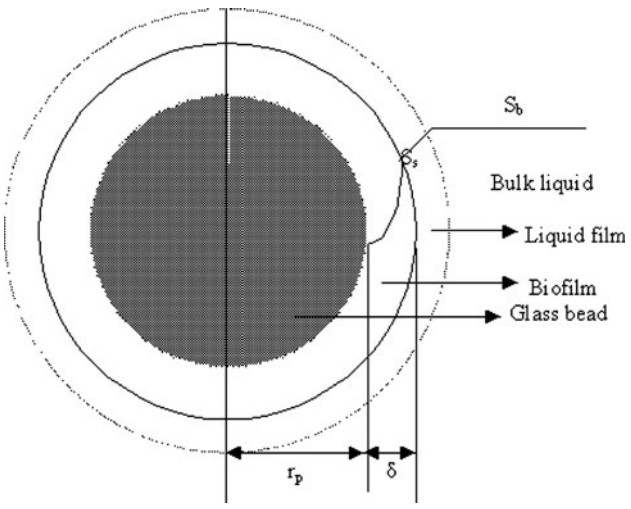

Fig. 1 Conceptual concentration profile at bioparticle interface in which external mass transport takes place through a stagnant liquid film and diffusive transport through the biofilm

5. Phenol is the only growth-limiting nutrient. Oxygen and all the other nutrients are present in excess. The critical oxygen concentrations for microorganisms generally lie in the range of 0.096–1.6 mg/L [11]. Concentration of dissolved oxygen (DO) in the reactor at steady state was found to be constant at 5.6 ± 0.4 mg/L. It is much greater than the range of critical oxygen concentrations for biological treatment processes, so that oxygen is not the rate limiting nutrient.
6. The growth kinetics follows Haldane-type substrate-inhibited kinetics with respect to phenol. The specific growth rate as a function of phenol concentration is thus:

$$\mu = \frac{\mu_m S}{(S + K_S + S^2/K_I)} \tag{1}$$

The consumption of substrates for cell maintenance energy is assumed to be insignificant.

7. Immobilisation of the cells into the biofilm does not alter the growth characteristics of the organism owing to microenvironmental conditions prevailing in the biofilm. So the growth kinetics obtained under batch conditions with free cells is applicable to immobilised cells also.
8. The effects of outward diffusion of metabolic products are negligible.
9. The diffusivity of phenol in the biofilm is assumed to be constant, independent of radial position in the biofilm and of the concentrations of phenol along the biofilm.

A steady-state mass balance over a thin shell of the biofilm leads to the following equations describing the concentration profile of phenol:

$$D_{\text{eff}}\left[\frac{d^2S}{dr^2} + \frac{2}{r}\left(\frac{dS}{dr}\right)\right] = \frac{\rho_b}{Y_{x/s}}\frac{\mu_{\max} S}{(S + K_S + S^2/K_I)} \tag{2}$$

The boundary conditions for this equation are:

$$\left(\frac{dS}{dr}\right) = 0 \quad \text{at } r = r_p \tag{3}$$

$$D_{\text{eff}}\left(\frac{dS}{dr}\right) = k_s(S_b - S_S) \quad \text{at } r = r_p + \delta \tag{4}$$

Equations (3)–(5) can be rewritten in terms of dimensionless variables as follows:

$$\frac{d^2S^*}{dx^2} + \frac{2}{\left(x + \frac{r_p}{\delta}\right)}\frac{dS^*}{dx} = \phi_s^2\frac{S^*}{\left(S^* + K_S^* + S^{*2}/K_I^*\right)} \tag{5}$$

$$\frac{dS^*}{dx} = 0 \quad \text{at } x = 0 \tag{6}$$

$$\frac{dS^*}{dx} = Bi(1 - S^*) \quad \text{at } x = 1.0 \tag{7}$$

where

$$S^* = \frac{S}{S_b} \quad x = \frac{r - r_p}{\delta} \quad K_S^* = \frac{K_S}{S_b} \quad K_I^* = \frac{K_I}{S_b}$$

$$\phi_s^2 = \frac{\rho_b \mu_{max} \delta^2}{Y_{x/s} D_{eff} S_b} \quad Bi = \frac{k_s \delta}{D_{eff}}$$

The flux at the surface of bioparticles can be calculated after solving Eqs. (5)–(7), and the overall phenol removal rate (R_s) can be found by multiplying the flux with the total surface area of bioparticles in the reactor (A_p)as given in Eq.(8).

$$R_s = A_p k_s (S_b - S_s) = A_p D_{eff} \left(\frac{dS}{dr}\right)_{r=r_9+\delta} \tag{8}$$

where $A_p = N_p\, 4\pi(r_p + \delta)^2$

The rate thus calculated is equivalent to that which can be found by integrating the reaction rate over the biofilm for a single bioparticle and multiplying by the number of particles in the reactor, i.e.

$$R_s = \frac{N_p \rho_b}{Y_{x/s}} \int_{r=r_p}^{r=r_p+\delta} \frac{\mu_{max} S}{(S + K_s + S^2/K_I)} 4\pi r^2 dr \tag{9}$$

Based on the complete mixing and steady-state approximations, as well as considering negligible phenol degradation in the bulk liquid phase, the mass balance of phenol over PPBR can be written as:

$$R_s = Q(S_I - S_b) = k_s A_p (S_b - S_s) \tag{10}$$

Using this set of model equations, bulk phenol concentration (S_b) in the reactor can be predicted. It is possible to find a value for S_b, which satisfies Eq. (10), by trial and error method, after solving Eqs.(5)–(7). The percentage degradation obtained using the model predicted value of S_b can be compared to that obtained using the experimentally measured value.

Solution method

Equation (5) is a second-order, nonlinear, ordinary differential equation with Eqs. (6) and (7) representing the boundary conditions. It is a split boundary value problem. This second-order, nonlinear, ordinary differential equation is rewritten as a set of two-first order ordinary differential equations:

$$\frac{dS^*}{dx} = y* \tag{11}$$

$$\frac{dy^*}{dx} = \phi_s^2 \frac{S^*}{\left(S^* + K_S^* + S^{*2}/K_I^*\right)} - \frac{2}{\left(x + \frac{r_p}{\delta}\right)} y* \tag{12}$$

These equations were solved by fourth–fifth order Runge–Kutta method using MATLAB version 6.5 as an initial value problem with shooting system technique [15] for one unknown initial condition. As the dimensionless parameters $\left(K_S, K_I, Bi, \varphi_s^2\right)$in the model need a value of S_b, a trial and error method was used. A value for S_b was assumed. Dimensionless parameters in the model were calculated. Then a value of S^* at $x = 0$ was assumed [let $S^*(x = 0) = a$]. With $S^*(x = 0)$ and y^* at $x = 0$ as the initial boundary conditions, Eqs. (11) and (12) were solved. S^* and y^* at any x could be obtained. The solution was marched forward using Eqs. (11) and (12), until Eq. (7) was satisfied. A new value of S^* at $x = 0$ for every iteration was calculated using Eq. (13):

$$a_{n+1} = a_n + \left[\frac{Bi(1 - S^*_{x=1})_n - (y^*_{x=1})_n}{\left(\frac{\partial y^*}{\partial a}\right)_{x=1}\Big|_n}\right] \tag{13}$$

To calculate the partial derivative $\left(\frac{\partial y^*}{\partial a}\right)_{x=1}$, shooting system dynamics for the unknown initial condition was defined as given by Ramirez [15]. The state equations, Eqs. (11) and (12), and shooting systems were solved simultaneously and the new initial condition a_{n+1} was calculated using Eq. (13). When Eq. (7) was satisfied, then the iteration for S^* was stopped for an assumed value of S_b. When Eq. (10) was satisfied, with the assumed value of S_b and with the value of S_s calculated from the solution of equations thereof, then the assumed value of S_b was taken as the bulk phenol concentration predicted from the model equations. Hence, the value for S_b, which satisfies Eq. (10), was calculated.

Materials and methods

Microorganism

Nocardia hydrocarbonoxydans (NCIM 2386) was obtained from NCIM, a division of National Chemical Laboratories, Pune, India. The strains were periodically subcultured once in 15 days on agar slants and stored at 4 °C.

Growth media

The organisms were grown on phenol as the sole carbon and energy source, and a nutrient medium of the following composition was used: ammonium nitrate (1 g/L), ammonium sulphate (0.50 g/L), sodium chloride (0.50 g/L), dipotassium hydrogen orthophosphate (1.5 g/L), potassium

dihydrogen orthophosphate (0.5 g/L), ferrous sulphate (0.002 g/L), calcium chloride (0.01 g/L) and magnesium sulphate (0.50 g/L) in distilled water. The solution was adjusted to pH 7.0 ± 0.1. For continuous experiments, nutrient media were prepared in tap water and sterile conditions were not used.

Acclimatised inoculum preparation

Organisms were acclimatised for the phenol concentrations of 100, 200, 300, 400, 500, 600, 800 and 900 mg/L gradually, according to the procedure explained elsewhere [10]. For acclimatisation at 10, 20, 40 and 60 mg/L phenol, a loopful of organisms from freshly subcultured slants was directly inoculated into flasks containing 100 ml of 10, 20, 40 and 60 mg/L phenol and all the required nutrients. The culture was kept in a shaker at 120 rpm and at 30± 1°C for 3 days. This formed the primary culture. The secondary acclimatised inoculum was prepared in the same way, wherein 1 mL of primary culture was used instead of the subculture to inoculate the medium, and the culture was incubated for 48 h. This was continued for the third and fourth acclimatisation. Cultures acclimatised for 10, 20, 40 and 60 mg/L were thus obtained. Acclimatised cultures were then stored at 4 °C.

Cell immobilisation

Cell immobilisation on glass beads of 3 mm size was done through attachment of cells, by using the cell suspension acclimatised to the corresponding phenol concentration, according to the procedure explained elsewhere [10].

Determination of biomass dry weight, biofilm thickness and biofilm density

The attached biomass dry weight in the reactor at steady state was measured by weight difference between the biomass-laden particles and the bare glass beads. The average biofilm thickness on the glass beads was measured using a Labomed optical microscope fitted with a dial micrometer. The detailed procedure for the estimation of attached biomass dry weight in the reactor and the biofilm thickness on the glass beads are described elsewhere [10]. The biofilm density was calculated based on the following equation [11]:

$$\rho_b = \frac{W}{N_p(\pi/6)\left[(d_p + 2\delta)^3 - d_p^3\right]} \quad (14)$$

Estimation of suspended cell concentration:

Suspended cell concentrations were determined by the measurement of absorbance at a wavelength of 610 nm using Hitachi UV spectrophotometer and then using a calibration of absorbance versus suspended cell concentrations in milligram biomass per litre. Suspended cell concentrations for calibration were obtained by dry weight measurement after filtering the cell suspensions of known dilutions through a 0.22-μm filter paper.

Phenol analysis

Phenol concentration was analysed by direct photometric method using 4-aminoantipyrene and measuring the absorbance at 510 nm with Hitachi UV spectrophotometer [16]. The samples were filtered through a 0.22 μm filter paper to remove any biomass before phenol analysis.

Growth kinetics of *Nocardia hydrocarbonoxydans* (Nc*h*) as suspended culture on phenol

Growth kinetic data for suspended cells of *Nch*. growing on phenol was obtained from batch growth experiments. Shake flask experiments were conducted to obtain the specific growth rates of *Nch.* at different initial phenol concentrations at a temperature of 30 ± 1 °C and initial pH of 7.0 ± 0.1. Phenol was used at a range of initial concentrations (10–500 mg/L) in 250 mL shake flasks containing 49 mL of the growth media prepared in sterilised distilled water and containing all the required nutrients and phenol at the required concentrations. As inoculum, 1 mL of cell suspension, which was four times acclimatised to the corresponding phenol concentration, was added to the flasks. A number of flasks, each containing 50 mL of the media and with the same initial phenol concentration, were placed in a shaker at 120 rpm speed, at the same time and at room temperature of 30 ± 1 °C. The flasks, one each at a time, were removed at different intervals of times and the samples were analysed for suspended cell concentrations. This was done to avoid the volume change, which occurs by removing the sample from the same flask at different time intervals.

Determination of yield coefficients

The value of yield coefficient, $Y_{x/s}$ was determined in batch culture using the shake flask experiments conducted at 100 mg/L initial phenol concentration. The observed yield coefficient was calculated as [17]

$$Y_{x/s} = \frac{\Delta X}{\Delta S} \quad (15)$$

where ΔX and ΔS are the change in biomass concentration and substrate concentration during the batch growth period.

Pulsed plate bioreactor

Experimental pulsed plate bioreactor is a cylindrical column consisting of a stack of five perforated plates with a plate spacing of 3 cm, mounted on a central shaft, and the entire stack of plates is reciprocated by a variable drive motor. The entire circumference of the plate stack was covered with a nylon mesh. A schematic representation and discussion of the experimental setup and operation of the pulsed plate bioreactor are presented elsewhere [10]. The space between the plates, forming each stage in the bioreactor, was filled with 1,600 (approximately 40 g) glass beads of 3 mm diameter, immobilised with *Nch*. Hence, the reactor consisted of four stages and 6,400 glass beads with immobilised cells. The volume of the reactor was 0.977 l. Synthetic phenol solution in tap water, with phenol at the required concentration, and all the other nutrients was pumped from the bottom using a peristaltic pump at the required flow rates. Compressed air was continuously passed from the bottom through a constant pressure regulator and a rotameter, at 1.7–1.8 L per min (LPM) to ensure proper supply of oxygen to the microorganisms. The frequency of pulsation (f) was set at 0.5 s^{-1} using the variable voltage speed regulator, and the amplitude (A) was set at 4.7 cm, by positioning the crankshaft. The concentration of phenol in the effluent from the column was analysed at regular intervals of time during start-up till steady state was attained. Steady-state conditions were assumed to exist in the system when phenol concentration in the effluent remained constant over a 12-h period. Eight such steady states were established and the conditions prevailing in each are given in Table 1. The time required to attain steady state (start-up time) in these eight runs varied from 24 to 40 h [18].

Determination of liquid–solid mass transfer coefficients

The knowledge of liquid–solid mass transfer coefficient for a pulsed plate bioreactor with a fixed bed of glass beads is essential for successful application of the mathematical model. The liquid–solid mass transfer coefficient for a pulsed plate column with a fixed bed of bare glass beads (without immobilised cells), in each stage formed by interplate spaces (1,600 beads/stage), was determined experimentally by benzoic acid dissolution method [19, 20] under air and liquid flow rates and pulsing conditions of interest (those used for steady-state biodegradation experiments). Solid benzoic acid cylinders of 4-mm diameter and 4-mm height were made by using a precisely machined aluminium mould with semi-cylindrical holes in each half of the mould. Benzoic acid powder was melted and poured into the mould and cooled; the mould was separated into two parts to remove the cylinder. The final size was adjusted by measuring with vernier calipers and smoothening with sandpaper.

A single active benzoic acid particle was placed between the shaft and the mesh covering of the plate stack in a particular stage, amidst the fixed bed of bare glass beads. Frequency and amplitudes of pulsation were set and tap water was poured into the reactor, up to the reactor volume. Immediately, tap water was pumped from the bottom using a peristaltic pump at the required rate, and the compressed air was passed at a rate identical to that used in the biodegradation experiments. The particle was allowed to remain inside the bed for a known time (retention time for benzoic acid particle in the column). At the end of this time period (experimental run time), the water flow, airflow and the pulsations were stopped simultaneously and the water was drained from the column. The time taken to start the run, after filling the column with water, was less than 20 s; for draining the water after the run, it was less than 15 s. The benzoic acid particle was then removed from the bed, dried and weighed with a microgram balance. The actual weight loss of the particle was measured. The particle retained its shape and the surface area of the particle decreased by less than 5% during a run. Hence, the surface area could be assumed to be constant and equal to the average of the areas before and after the run. The benzoic acid concentration in the drained liquid from the reactor was measured by titration with 0.001 M NaOH solution. The dissolution of a single benzoic acid particle had a negligible effect on the concentration of dissolved benzoic acid. The concentration of benzoic acid in the liquid (C) was approximately 8–9 mg/L in various runs. The mass transfer rate (or weight loss per unit area per unit time) could then be obtained and the mass transfer coefficient was computed with the following equation:

$$(\Delta m/\Delta t)/a_{\text{avg}} = k_{\text{s}}(C^{*} - C) \tag{16}$$

where C^{*} is the solubility of benzoic acid in water at 30 °C, obtained by using the correlation given by Guedes et al. [21].

Table 1 Operating conditions at different steady-state runs

Steady-state run no.	Q (mL h^{-1})	A (cm)	f (s^{-1})	Air flow rate (LPM)	S_{I} (mg/L)
1	400	4.7	0.5	1.7–1.8	800
2	600	4.7	0.5	1.7–1.8	800
3	800	4.7	0.5	1.7–1.8	800
4	1,000	4.7	0.5	1.7–1.8	800
5	400	4.7	0.5	1.7–1.8	900
6	600	4.7	0.5	1.7–1.8	900
7	800	4.7	0.5	1.7–1.8	900
8	1,000	4.7	0.5	1.7–1.8	900

For each operating condition of interest, separate experiments were performed by placing a single benzoic acid particle in any given stage (1st, 2nd, 3rd or 4th stages) for different experimental run times (150, 300, 450 and 600 s). A smaller experimental run time minimises the error due to the changing surface area of the particle, while a larger run time minimises the error due to dissolution of benzoic acid during the start-up and shutdown period of the experiment ($\approx$35 s). Then mass transfer coefficient for a given stage was calculated with each experimental run time. The mass transfer coefficients obtained with different experimental run times, for a case with benzoic acid particle in a particular stage(e.g. 2nd stage), were averaged to get the mass transfer coefficient for that stage (2nd stage). Since identical mixing conditions prevail in the entire reactor, the average mass transfer coefficient for the entire reactor was obtained by averaging the local mass transfer coefficients calculated for each stage (1st, 2nd, 3rd and 4th), by performing separate runs with a benzoic acid particle at different stages. All the experimental runs were duplicated, and less than 1% error in the mass transfer coefficients was obtained in duplicate runs.

Results and discussion

Evaluation of microbial growth kinetic parameters from shake flask experimental data

The time course variations of suspended biomass concentration for different initial phenol concentrations are shown in Figs. 2 and 3. The specific growth rates of *Nch.* at different initial phenol concentrations were determined from the slope of the plot of $\log_e$ (suspended biomass concentration) against time for the exponential growth phase. The specific growth rates thus obtained at different initial phenol concentrations were fitted by the Haldane equation, using the curve-fitting tool of MATLAB version 6.5. The fit of the Haldane equation with correlation coefficient of 0.9097 is shown in Fig. 4. The biokinetic parameters derived for a temperature of 30 ± 1 °C are: $\mu_m = 0.5397\ h^{-1}$, $K_S = 6.445$ mg/L and $K_I = 855.7$ mg/L. The maximum specific growth rate occurs at a phenol concentration (S_{max}) equal to $\sqrt{K_S K_I}$ [17] for the Haldane-type growth kinetics and was found to be 74.26 mg/L. It shows that the substrate inhibition of *Nch.* occurs at phenol concentrations greater than 74.26 mg/L. This concentration is greater than the inhibitory level of phenol to many other phenol-degrading organisms shown in Table 2. The table shows the growth kinetic parameters for different phenol-degrading organisms reported in literature. S_{max} values that are given in Table 2 are calculated using the reported growth kinetic parameters.

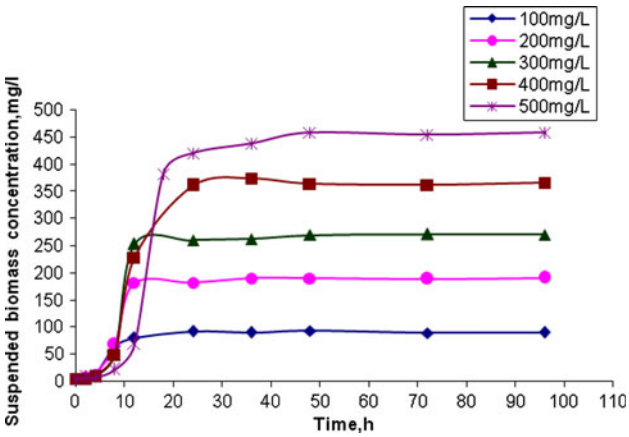

Fig. 3 Batch kinetic data on the variation of suspended biomass concentration

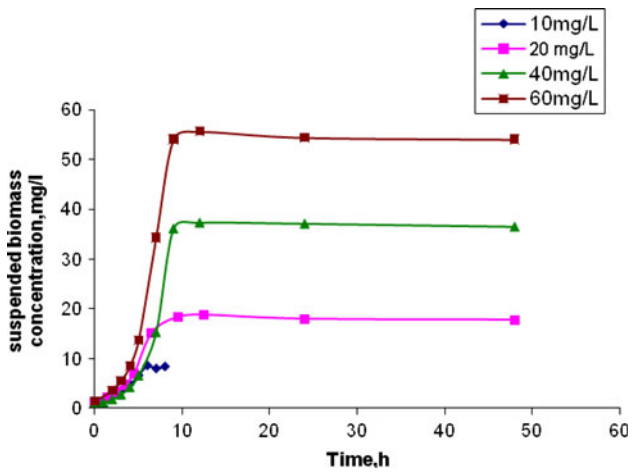

Fig. 2 Batch kinetic data on the variation of suspended biomass concentration

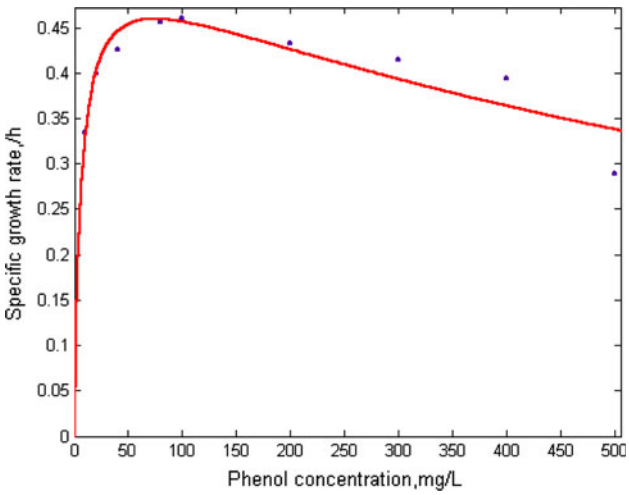

Fig. 4 Specific growth rate as a function of phenol concentration fitted by the Haldane model

Table 2 Microbial strains capable of degrading phenol

Culture	T (°C)	pH	μ_m (h^{-1})	K_S (mg/L)	K_I (mg/L)	S_{max} (mg/L)	Reference
P. putida CCRC14365	30	6.8	0.33	13.9	669	96.43	[4]
P. putida DSM 548	26	6.8	0.436	6.19	54.1	18.3	[22]
P. putida ATCC49451	–	–	0.9	6.93	284.3	44.39	[23]
P. putida ATCC17514	30	6.0	0.567	2.38	106	15.88	[24]
P. putidaATCC 700007	30	7	0.051	18	430	87.98	[25]
P. fluoroescens	–	–	0.618	71.4	241	131.18	[26]
Acinetobacter	30	–	0.83	1.5	250	19.36	[27]
Trichosporon cutaneum R57	–	–	0.42	110	380	204.45	[28]
Candida tropicalis	–	–	0.48	11.7	207.9	49.32	[29]
Nocardia hydrocarbonoxydans	30 ± 1	7 ± 0.1	0.5397	6.445	855.7	74.26	This study

S_{max} values were calculated using K_s and K_I values reported in columns 5 and 6, respectively $S_{max}=\sqrt{K_s K_I}$.

Figures 3 and 5 show the time course variations of biomass and phenol concentrations, respectively, during shake flask experiments at 100 mg/L initial phenol concentration in the batch growth period. The yield coefficient, $Y_{x/s}$ in this study, using the data from Figs. 3 and 5, was 0.86 mg cells formed per milligram of phenol consumed. The growth yield coefficients for other pure and mixed cultures growing on phenol, reported in literature, ranged from 0.45 to 0.85 [11, 12, 24, 30–32]. The growth yield coefficient of *Nch.* on phenol, obtained in the present study, was comparatively higher. S_{max} and K_I values for *Nch.* in this study are comparatively higher than those for many of the phenol-degrading organisms cited in Table 2. It shows that the inhibition effect of phenol on *Nch.* is less than that for many other organisms. Higher $Y_{x/s}$, S_{max} and K_I values show that *Nch.* can be a substitute for many microorganisms used for biodegradation of phenol at low concentrations and may be even preferred when the phenol concentration is high.

Liquid–solid mass transfer coefficient

The results of the experiments performed to determine the liquid–solid mass transfer coefficient (k_s) at the same operating conditions (air and liquid flow rates, amplitude and frequency of pulsation) as used in steady-state biodegradation runs are given in Table 3. Table 3 shows the values of k_s obtained by averaging the individual k_s values obtained for four stages. Liquid–solid mass transfer coefficients for PPBR are found to be higher than those for three-phase packed bed bioreactors [33, 34] and of similar range as for fluidised bed bioreactors [11, 35, 36].

Steady-state phenol degradation

The percentage degradation, attached biomass dry weight, average biofilm thickness and biofilm density at steady state, obtained for eight steady-state runs, are shown in Table 4.

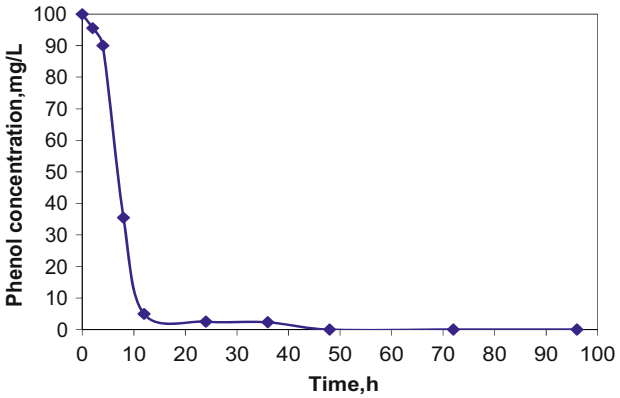

Fig. 5 Time course variation of phenol concentration at 100 mg/L initial phenol concentration: batch data

Table 3 Mass transfer coefficients at different operating conditions

Q (mL h^{-1})	A (cm)	f (s^{-1})	Air flow rate (LPM)	$k_s \times 10^5$ (m s^{-1})
400	4.7	0.5	1.7–1.8	5.45
600	4.7	0.5	1.7–1.8	5.86
800	4.7	0.5	1.7–1.8	5.94
1,000	4.7	0.5	1.7–1.8	6.0

The mathematical model equation (5) along with the boundary conditions (6) and (7) has been solved by fourth–fifth order Runge–Kutta method as an initial value problem using shooting system technique. Liquid–solid mass transfer coefficients for pulsed plate column obtained by benzoic acid dissolution method were used in the PPBR model equations. Growth kinetic parameters obtained by batch experiments were incorporated into the kinetic term of the model equation. Another parameter required for model simulation is the effective diffusivity of phenol in the biofilm (D_{eff}). D_{eff} is obtained by multiplying the diffusivity of phenol in the bulk liquid phase (D_w), by a factor to correct

Table 4 Results of steady-state biodegradation

Run no.	Biomass dry weight (kg $\times 10^3$)	δ (m $\times 10^6$)	ρ_b (kg m^{-3})	Percentage degradation (experimental)	Percentage degradation (calculated)	% Absolute error
1	6.63	74.4	468.7	97.04	98.27	1.27
2	4.74	61.3	410.4	96.99	97.42	0.44
3	3.67	55.9	349	96.63	96.24	0.4
4	3.26	53.7	324.2	94	94.99	1.05
5	2.49	103.4	124.2	96.6	97.25	0.67
6	2.2	82	140	95.59	95.7	0.115
7	1.91	66.8	151.4	94.56	93.83	0.77
8	1.79	60.2	158	93.23	91.34	2

the additional diffusional resistance in the biofilm. The range of D_{eff}/D_w for phenol within various biofilms was found to vary from 7 to 88% [11, 12, 36, 37]. Diffusivity of phenol in water at 30 °C was calculated to be 1.1×10^{-9} m^2 s^{-1} using the Wilke–Chang correlation [38]. In the present study, the effective diffusivity was taken as 80% of that in water at 30 °C [34, 37].The model parameters used in solving the equation are shown in Table 5.

Bulk phenol concentrations and percentage degradation of phenol were calculated by model simulation. These predicted values of percentage degradation were compared with the experimentally observed values. Such a comparison for eight steady-state runs is shown in Table 4. Maximum deviation between the experimental values and those calculated from the model is found to be 2%, thereby showing the validation of the model for pulsed plate bioreactor.

The concentration profiles of phenol within the biofilm are obtained by simulating the biofilm model equations using the experimentally measured values of bulk concentrations and the boundary conditions specified. The corresponding concentrations at the surface of the biofilm (S_s) were also obtained from the model simulation. The representative plots of the concentration profiles in the biofilm for runs 2 and 6 are shown in Figs. 6 and 7, respectively. Table 6 shows the concentration of phenol in the bulk liquid phase (S_b), at the surface of the biofilm ($S_s = S_{x=1}$) and at the surface of the glass particle ($S_{x=0}$). For all the steady-state runs, S at $x = 0$ is greater than zero. It shows that the entire depth of the biofilm may be active, owing to substrate availability. It is also seen that the concentration near the surface of glass beads are very near to zero in most of the runs.

Three effectiveness factors can be defined for this system as shown in Eqs. 18–20 [39], where

$$\text{Substrate consumption rate} = \mathrm{R}\,(S) = \frac{W\mu_m S}{Y_{x/s}\left(K_S + S + \frac{S^2}{K_I}\right)} \tag{17}$$

$$\eta_{overall} = \frac{\text{Observed reaction rate}}{\text{Reaction rate if not slowed down by internal diffusion or external mass transfer resistance}} = \frac{Q(S_I - S_b)}{R(S_b)} \tag{18}$$

$$\eta_{imternal} = \frac{\text{Observed reaction rate}}{\text{Reaction rate if not slowed down by internal diffusion, but in the presence of external mass transfer limitations}} = \frac{Q(S_I - S_b)}{R(S_S)} \tag{19}$$

$$\eta_{\text{external}} = \frac{R(S_S)}{R(S_b)} = \frac{\text{Reaction rate if not slowed down by internal diffusion, but in the presence of external mass transfer limitations}}{\text{Reaction rate if not slowed down by internal diffusion or external mass transfer resistance}} \quad (20)$$

The effectiveness factors calculated for different runs are shown in Table 6.

The effectiveness factors are related by

$$\eta_{\text{overall}} = \eta_{\text{internal}} \cdot \eta_{\text{external}} \quad (21)$$

The external effectiveness factor varies from approximately 0.78 to 0.98 in the eight runs. η_{external} increases with the flow rate and $\eta_{\text{external}} \rightarrow 1$ as the flow rate increases. This shows that the resistance offered by external liquid film becomes less significant with the increase in flow rate. η_{internal} varies from 0.12 to 0.89. The values of overall effectiveness factors (η_{overall}) vary from 0.097 to 0.87 and these values are found to be closer to the respective η_{internal} values. This shows that the performance of the cells in the biofilm, biodegradation rate and hence the reactor performance are mainly governed by internal diffusion limitations, rather than the external mass transfer resistance.

η_{overall} increased with increase in flow rate and increase in inlet concentrations. As the flow rate increases, $\eta_{\text{external}} \rightarrow 1$. At 900 ppm inlet concentration, η_{external} values are closer to 1 than at 800 ppm inlet concentration. This implies that as the flow rate or inlet phenol concentration increases, contribution of external film resistance to the overall transport resistance decreases. So the concentration at the biofilm surface will be closer to bulk substrate concentrations. Hence, the biomass at the surface of the biofilm is exposed to higher phenol concentrations and so the biomass at the interiors of the biofilm will also be exposed to higher phenol concentrations. As long as the increased phenol concentrations encountered by the biomass are not inhibitory (as observed in these runs), the

Table 5 Model parameters

Parameter	Value	Source
D_{eff}	8.8×10^{-10} m^2 s^{-1}	Assumed (=0.8 D_w)
μ_{max}	1.499×10^{-4} s^{-1}	Shake flask experiment
K_S	6.445×10^{-3} kg m^{-3}	Shake flask experiment
K_I	855.7×10^{-3} kg m^{-3}	Shake flask experiment
$Y_{X/S}$	0.86 kg kg^{-1}	Shake flask experiment
ks	Shown in Table 2 m s^{-1}	Benzoic acid dissolution experiment
N_p	6400	Number of glass beads used in bioreactor
r_p	1.5×10^{-3} m	Radius of glass beads used
δ	Shown in Table 4 m	Determined using microscope
ρ_b	Shown in Table 4 kg m^{-3}	Determined using Eq. (14)

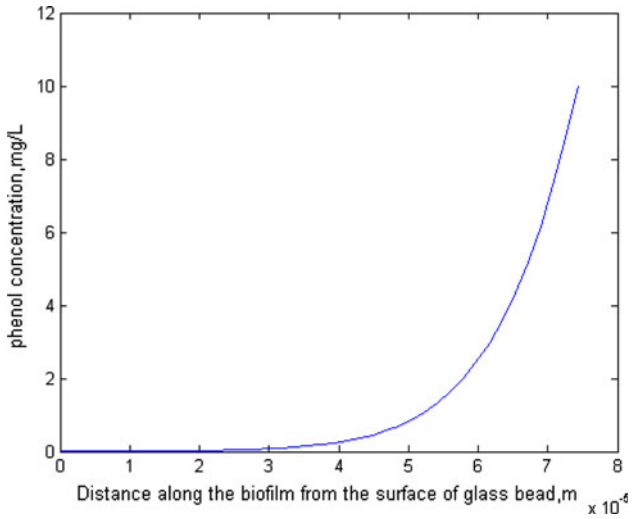

Fig. 6 Concentration profile in the biofilm at $S_I = 800$ mg/L; $Q = 400$ mL/h; $A = 4.7$ cm; $f = 0.5$ s^{-1}

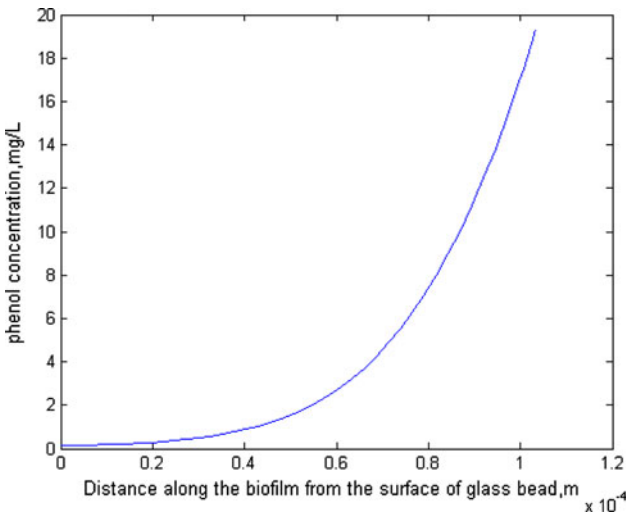

Fig. 7 Concentration profile in the biofilm at $S_I = 900$ mg/L; $Q = 400$ mL/h; $A = 4.7$ cm; $f = 0.5$ s^{-1}

Table 6 Phenol concentrations and dimensionless parameters

Run no.	S_b (mg/L)	$S_s = S_{x=1}$ (mg/L)	$S_{x=0}$ (mg/L)	Bi	η overall	η internal	η external	φ_s	$Da \times 10^{16}$
1	23.72	10.01	0.004	4.61	0.0971	0.1237	0.7847	4.6537	5.97
2	24.1	11.14	0.0039	4.08	0.2030	0.2494	0.8141	3.5595	4.58
3	26.96	13.44	0.153	3.78	0.3415	0.4019	0.8496	2.8348	3.99
4	48	27.13	0.802	3.66	0.4376	0.4667	0.9378	1.9624	6.37
5	30.6	19.33	0.157	6.41	0.2780	0.3024	0.9191	2.9307	2.99
6	39.7	26.08	0.734	5.46	0.4520	0.4777	0.9461	2.1708	3.6
7	48.9	32.89	2.81	4.50	0.6754	0.7013	0.9631	1.6530	3.8
8	60.9	42.53	7.59	4.10	0.8797	0.8979	0.9788	1.3637	4.47

observed reaction rate increases with the increase in flow rate or inlet phenol concentration. So, $\eta_{overall}$ increases with increase in flow rate and inlet phenol concentration. But in all the runs, $\eta_{external}$ values are less than 1. This shows that though the effect of external mass transfer resistance is less as compared with internal diffusional resistance, the external film resistance cannot be neglected.

The values of Biot number (Bi), Thiele modulus (φ_s) and Damkohler number calculated for the eight steady-state runs are also shown in Table 6. Biot number is a ratio of the external mass transfer rate to the internal mass transfer rate. The values of $Bi > 1$ show that the effects of internal diffusional limitations are more pronounced than the external mass transfer limitations. But the difference between S_b and S_s values in Table 5 and $\eta_{external}$ values in Table 4 show that external liquid–solid mass transfer resistance also accounts for a large portion of the transport resistance.

Square of Theile modulus (φ_s^2) is the ratio of the rate of removal of substrate by reaction to the rate of diffusion of the substrate. Thiele modulus (φ_s) values vary from 1.36 to 4.65 and hence φ_s^2 values vary from 1.85 to 21.62. Biochemical reaction rate is higher than the internal diffusion rate showing that internal diffusional resistance is significant. Theile modulus has decreased with increase in flow rate or influent concentration. This shows that the internal diffusional resistance reduces with increase in flow rate or influent concentration.

Damkohler number (Da) is designated as the ratio of maximum rate of substrate consumption to the maximum rate of external mass transfer.

$$Da = \frac{\mu_m \rho_v / Y_{x/s}}{\left[k_s 4\pi (r_p + \delta)^2 S_b\right] / \frac{\pi}{6}\left[(2r_p + 2\delta)^3 - 8r_p^3\right]} \quad (22)$$

In all the steady-state runs, Da is in the range of 2.99×10^{-16} to 6.37×10^{-16}. So, $Da << 1$ indicates that maximum reaction rate (rate of substrate consumption or biodegradation) is much less than the maximum external mass transfer rate and hence external mass transfer limitations are negligible as compared with the reaction limitations.

From the above discussions based on effectiveness factors and various dimensionless numbers, it is evident that the biofilm internal diffusion rate is the slowest step in the process of biodegradation of phenol by immobilised *Nocardia hydrocarbonoxydans* in a pulsed plate bioreactor. Biofilm characteristics is a main decisive factor governing internal diffusion rate as compared to reactor type. So enhancing internal diffusion rate can be done mainly by improving biofilm characteristics.

Conclusions

The growth of *Nocardia hydrocarbonoxydans* on phenol was found to follow the Haldane substrate inhibition model. The biokinetic parameters at a temperature of 30 ± 1 °C and pH at 7.0 ± 0.1 are $\mu_m = 0.5397\ h^{-1}$, $K_S = 6.445$ mg/L and $K_I = 855.7$ mg/L. The substrate inhibition of *Nch.* occurs at phenol concentrations greater than 74.26 ppm. The yield coefficient, $Y_{x/s}$, obtained in this study was 0.86 mg cells formed per milligram phenol consumed.

A mathematical model has been used to describe the steady-state biodegradation of phenolic wastewater in a pulsed plate bioreactor consisting of the cells of *Nocardia hydrocarbonoxydans* immobilised on glass beads. The model considers the simultaneous diffusion and reaction of phenol within the biofilm and the external mass transfer resistance between the biofilm and the completely mixed bulk liquid phase. The mathematical model was able to predict the performance of PPBR with immobilised cells very well, with a maximum error of 2% between the predicted and experimental percentage degradations of phenol.

From the effectiveness factors and various dimensionless numbers such as Biot number, Thiele modulus and Damkohler number, it is evident that the biofilm internal diffusion rate is the slowest step in the process of biodegradation of phenol by *Nocardia hydrocarbonoxydans* in a pulsed plate bioreactor.

References

1. Ehrhardt HM, Rehm HJ (1985) Phenol degradation by microorganisms adsorbed on activated carbon. Appl Microbiol Biotechnol 21:32–36
2. Prieto M, Hidalgo A, Serra JL, Llama MJ (2002) Degradation of phenol by *Rhodococcus erythropolis* UPV-1 immobilized on Biolite in a packed-bed reactor. J Biotechnol 97:1–11
3. Chen KC, Lin YH, Chen WH, Liu YC (2002) Degradation of phenol by PAA-immobilized *Candida tropicalis*. Enzyme Microb Technol 31:490–497
4. Chung TS, Tseng HY, Juang RS (2003) Mass transfer effect and intermediate detection for phenol degradation in immobilized *Pseudomonas putida* systems. Process Biochem 38:1497–1507
5. Mordocco A, Kuek C, Jenkins R (1999) Continuous degradation of phenol at low concentration using immobilized *Pseudomonas putida*. Enzyme Microb Technol 25:530–536
6. Tziotzios G, Teliou M, Kaltsouni V, Lyberatos G, Vayenas DV (2005) Biological phenol removal using suspended growth and packed bed reactors. Biochem Eng J 26:65–71
7. Pawlosky U, Howell JA (1973) Mixed culture biooxidation of phenol. 1. Determination of kinetic parameters. Biotechnol Bioeng 15:889–896
8. Dikshitulu S, Baltzis BC, Lewandowski GA, Pavlou S (1993) Competition between two microbial populations in a sequencing fed-batch reactor: theory, experimental verification, and implications for waste treatment applications. Biotechnol Bioeng 42:643–659
9. Dursun AY, Tepe O (2005) Internal mass transfer effect on biodegradation of phenol by Ca-alginate immobilized *Ralstonia eutropha*. J Hazard Mater B126:105–111
10. Shetty KV, Kalifathulla I, Srinikethan G (2007) Performance of pulsed plate bioreactor for biodegradation of phenol. J Hazard Mater 140:346–352
11. Tang WT, Fan LS (1987) Steady state phenol degradation in a draft-tube, gas–liquid–solid fluidized bed bioreactor. AIChE J 33:239–249
12. Livingston AG, Chase HA (1989) Modeling phenol degradation in a fluidized bed bioreactor. AIChE J 35:1980–1992
13. Vinod AV, Reddy GV (2005) Simulation of biodegradation process of phenolic waste water at higher concentrations in a fluidized-bed bioreactor. Biochem Eng J 24:1–10
14. Vidyavathi N (1998) Bioremediation of industrial and domestic effluents by microorganisms. PhD thesis, Department of Chemical Engineering, KREC Surathkal, Mangalore University, India
15. Ramirez WF (1989) Computational methods for process simulation. Butterworth Publishers, Stoneham, pp 295–297
16. AWWA, APHA, WEF (1975) Standard methods for the examination of water and wastewater, 14th edn. American Public Health Association/American Water Works Association/Water Environment Federation, Washington, p 580
17. Shuler ML, Kargi F (2002) Bioprocess engineering-basic concepts, 2nd edn. Prentice Hall of India, New Delhi, pp 73, 165
18. Shetty KV, Ramanjaneyulu R, Srinikethan G (2007) Biological phenol removal using immobilized cells in a pulsed plate bioreactor: effect of dilution rate and influent phenol concentration. J Hazard Mater 149:452–459
19. Prakash A, Briens CL, Bergougnou MA (1987) Mass transfer between solid particles and liquid in a three phase fluidized bed. Can J Chem Eng 65:228–236
20. Arters DC, Fan LS (1986) Solid–liquid mass transfer in a gas–liquid–solid fluidized bed. Chem Eng Sci 41:107–115
21. Guedes de Carvalho JRF, Delgado JMPQ, Alves MA (2004) Mass transfer between flowing fluid and sphere buried in packed bed of inerts. AIChE J 50:65–74
22. Monteiro AMG, Boaventura RAR, Rodrigues AE (2000) Phenol biodegradation by *Pseudomonas putida* DSM 548 in a batch reactor. Biochem Eng J 6:45–49
23. Wang SJ, Loh KC (1999) Modeling the role of metabolic intermediates in kinetics of phenol biodegradation. Enzyme Microb Technol 25:177–184
24. Yang RD, Humphrey AE (1975) Dynamic and steady state studies of phenol biodegradation in pure and mixed cultures. Biotechnol Bioeng 17:1211–1235
25. Abuhamed T, Bayraktar E, Mehmetoglu T, Mehemetoglu U (2004) Kinetics model for growth of *Pseudomonas putida* F1 during benzene, toluene and phenol biodegradation. Process Biochem 39:983–988
26. Kumaran P, Paruchuri YL (1997) Kinetics of phenol biotransformation. Water Res 31:11–22
27. Hao OJ, Kim MH, Seagren EA, Kim (2002) Kinetics of phenol and chlorophenol utilization by *Acinetobacter* species. Chemosphere 46:797–807
28. Alexievaa Z, Gerginova M, Zlateva P, Peneva N (2004) Comparison of growth kinetics and phenol metabolizing enzymes of *Trichosporon cutaneum* R57 and mutants with modified degradation abilities. Enzyme Microb Technol 34:242–247
29. Yan J, Jianping W, Hongmei L, Suliang Y, Zongding H (2005) The biodegradation of phenol at high initial concentration by the yeast *Candida tropicalis*. Biochem Eng J 24:243–247
30. Jones GL, Jansen F, McCay AJ (1973) Substrate inhibition of the growth of bacterium NCIB8250 by phenol. J Gen Microbiol 74:139–148
31. Pawlowsky V, Howell JA (1973) Mixed culture biooxidation of phenol. I. Determination of kinetic parameters. Biotechnol Bioeng 15:889–896
32. Hill GA, Robinson CW (1975) Substrate inhibition kinetics: Phenol degradation by *Pseudomonas putida*. Biotechnol Bioeng 17:1599–1615
33. Sheeja RY, Murugesan T (2002) Mass transfer studies on the biodegradation of phenols in up-flow packed bed reactors. J Hazard Mater B89:287–301
34. Hsien TY, Lin YH (2005) Biodegradation of phenolic wastewater in a fixed biofilm reactor. Biochem Eng J 27:95–103
35. Fan LS, Ramos RL, Wisecarver K, Zehner B (1990) Diffusion of phenol through a biofilm grown on activated carbon particles in a draft tube three phase fluidized bed bioreactor. Biotechnol Bioeng 35:279–286
36. Tang WT, Wisecarver K, Fan LS (1987) Dynamics of a draft tube gas–liquid–solid fluidized bed bioreactor for phenol degradation. Chem Eng Sci 42:2123–2134
37. Spigno G, Zilli M, Nicolella C (2004) Mathematical modeling and simulation of phenol degradation in biofilters. Biochem Eng J 19:267–275
38. Treybal RE (1980) Mass Transfer Operations. 3rd ed, McGraw-Hill International Editions–Chemical Engineering Series, Singapore, p 35
39. Open Universiteit1 (1992) The Netherlands and Thames Polytechnic, UK, Operational Modes of Bioreactors, BIOTOL Series, Butterworth Heinemann Ltd. Oxford